JOURNAL OF MATERIALS SCIENCE 33 (1998) 625–638

Craze testing for tough polyethylene

D.-M. DUAN, J. G. WILLIAMS
Department of Mechanical Engineering, Imperial College, London SW7 2BX, UK

It has been generally accepted that all the modes of fracture, including rapid crack growth, quasi-static fracture and slow crack growth in polyethylene are associated with the behaviour of the craze ahead of the crack tip. For recently developed tough pipe grade polyethylene materials, the need for knowledge of the craze behaviour seems particularly important in understanding the fracture behaviour of various modes since, with the low Young's moduli and low yield stresses, large craze zones tend to make it difficult to interpret the test data using a fracture mechanics approach. A novel test method is described in this paper which is designed for craze generation and craze behaviour analysis under plane strain conditions. The test method has been proved to be suitable both for quasi-static fractures and for long term fractures, and hopefully for rapid fractures, in tough polyethylene materials. The test data of yield stress against time to yielding show a clear brittle ductile transition which implies different fracture mechanisms in short term fracture and in long term fracture. © *1998 Chapman & Hall*

1. Introduction

With the increasing application of polyethylenes (PE) as structural materials, their fracture behaviour has received considerable attention over the last 20 years. Due to their high molecular weight and their time dependent characteristics, polyethylenes can exhibit various fracture modes depending on the loading conditions. While rapid, brittle crack propagation can occur in pipes under internal pressure [1, 2], ductile fractures can take place due to overloading or other reasons [3]. Another important failure phenomenon in polyethylene pipes are failures that occur after many years of service through a brittle slow crack growth mechanism [4, 5]. As in amorphous thermoplastics, polyethylenes exhibit a local rarefaction process known as "crazing" at high strain levels that occurs at crack tips, and it is generally accepted that all the modes of fracture in polyethylenes are intimately associated with the development of the crazed material as a precursor to fracture. It is also agreed that the fracture growth process consists of the failure of this crazed material, particularly for the slow crack growth mechanism [3, 4, 6–8].

With attention concentrated on the behaviour of the craze zone, slow crack growth problems have been investigated using various approaches ranging from microscopic modelling [9, 10] to phenomenological fracture mechanics [4]. The microscopic approach is directed at simulating the creep behaviour of the crazed material by investigating drawn material produced under plane stress conditions. The applicability of this approach is limited because the specimen size is not comparable with the craze zone and inevitably the stress distribution along the craze edge needs to be determined [11] which involves indirect measurement of the stresses. Fracture mechanics deals with the problems in such a way that it ignores the details of the events taking place in the craze zone and uses scaling parameters, K or J, of the stress field outside the zone to characterize the fracture behaviour. When the craze zone is engulfed in a stress field dominated zone, all the micro events happening in the zone can be regarded as being controlled by the macroscopic stress field. This approach has been successfully applied to brittle polymers during the last 20 years including the characterization of slow crack growth in high density polyethylenes. However, difficulties have been met in the fracture of tough polymers such as some more recent medium density tough polyethylenes [12, 13]. The first difficulty encountered is the achievement of plane strain fracture conditions under which a craze is generated in the specimen tested without pronounced crack tip blunting which usually occurs in a state of less constraint. Another difficulty is the interpretation of test data where fracture mechanics have proved to be inapplicable for the following reasons [14]: (a) the relatively low yield stress and low modulus lead to a large crack tip craze zone (up to 35% of the ligament length) which eliminates the stress singularity at the crack tip; (b) large load point deflections of the test pieces often violate the assumptions of the elastic analysis used; and (c) the coupling effect between the craze zone and stress redistribution along the ligament of a test piece (especially bending specimens) makes it difficult to evaluate the stress dependence of the craze behaviour.

In the latter case, as Kanninen [13] argued, detailed models of the craze need to be formulated to interpret the slow crack growth results. Following Kanninen's terminology, the brittle polyethylene materials which can be characterized by using fracture mechanics can be classified as category I and the more recent, tough,

materials as category II. The criterion of the classification is whether the craze length is less than 6% of the ligament length. The situation indicates that a better understanding of the fracture behaviour of these tough polyethylenes, especially of long term slow crack growth, must be based on an investigation of the crack tip craze zone and, at the same time, this zone should preferably be analysed under a constant level of stress rather than in a time dependent stress field. To achieve this end, two issues are raised. One is how to produce a craze zone experimentally under plane strain conditions and under a given stress. The craze zone produced should resemble the zone at a crack tip in real structures and the tests should provide accurate data. Although some methods have been developed for the tests of pipe grade polyethylenes [15, 16] using four notch specimens, which reduce the plane stress effect on the rupture strength measurement, these tests include crack growth as well as craze growth and therefore can not provide specific information on the craze behaviour. The other is how to choose an approach which is suitable for use in analysing the experimental results and therefore to model the material behaviour.

In this paper, a novel crazing test will be described which attempts to produce a craze in a specially designed specimen configuration and the basic mechanical behaviour of the craze will be presented and analysed. Based on the test results, the possible ways which can be used to characterize the craze damage behaviour will also be explored so as to evaluate the long term fracture resistance of the materials.

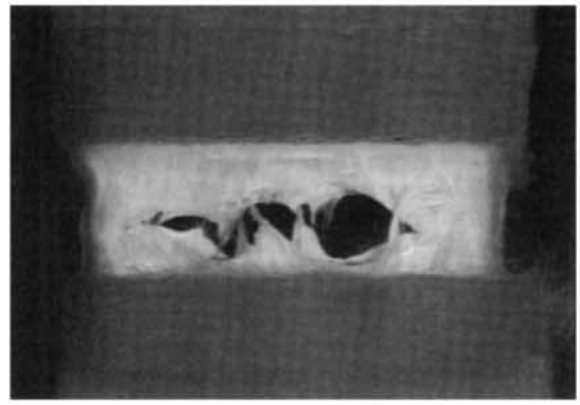

Figure 1 A side view of a deep double edge notched specimen showing plane stress effect in the near surface areas.

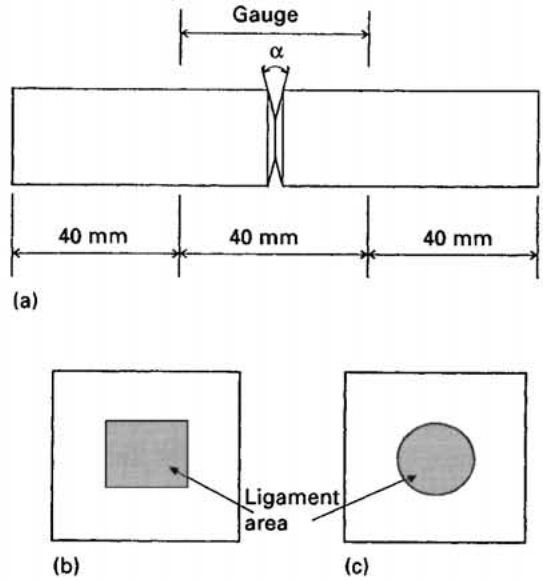

Figure 2 The craze test specimen geometry.

2. Experimental procedure

2.1. Experimental considerations

To produce a craze zone that resembles the one at a crack tip in polyethylene and to obtain reliable information both on the time dependence and stress dependence of zone growth and failure, several factors must be taken into account when a crazing test is designed. First of all, a craze zone at a crack tip is produced from the high local stress due to the geometrical discontinuities of the loaded structure rather than a high overall stress in the structure. Because polyethylenes show a high degree of non linearity and flow at high stresses [17], a deep notched specimen must be used so that a confined craze zone is produced with the bulk undergoing small strains which are easy to analyse. Secondly, to examine the stress dependence of the craze behaviour, the craze zone must initiate and grow under a definite stress rather than a time dependent stress field. Thus configurations undergoing bending deformation should be avoided since the stress redistribution tends to complicate the analysis. Thirdly, the completely different deformation behaviour of polyethylene under plane stress (necking) and plane strain (crazing) makes it essential for investigating the craze behaviour to minimize the influence of plane stress effects. Fig. 1 shows the plane stress effect in a deep double edge notched specimen (a side view) where the plane strain dominant part (central part) has already failed, but the two sides, where plane stress is dominant, are still bridged. This has led to the adoption of circumferentially deep notched tensile specimens.

2.2. Specimen and test apparatus

Circumferentially deep notched tensile (CDNT) specimens were fabricated from bars cut from compression moulded sheets. The bars had square cross-sections (20×20 mm) and were either rectangular notched or round notched as shown schematically in Fig. 2(a–c). The ligament area was generally about one tenth of the original cross-section. The notch angle was 45° for rectangular notches and 20° for round notches. The tip radius of the cutter for round notches was about 70 μm while the rectangular notches were sharpened by sliding into the root of the notch with a fresh razor blade of a tip radius $\rho < 20$ μm. Fig. 3 shows the crack tip quality of a round notched specimen which was centrally sectioned. The gauge length between the grips was 40 mm. If the gauge length is too small the stress state near the ligament plane will be influenced by the compression of the grips. On the other hand,

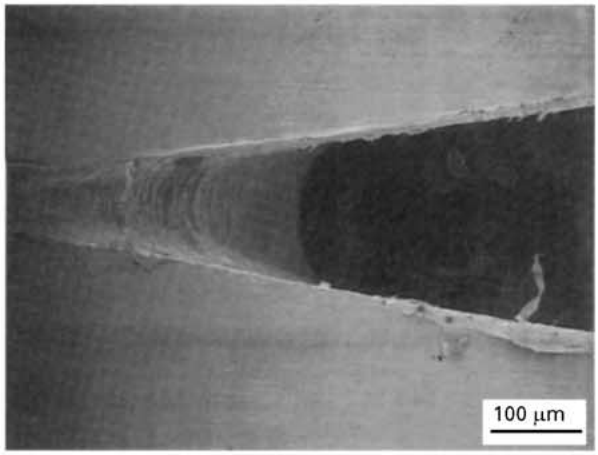

Figure 3 Notch tip quality for the round notched specimen.

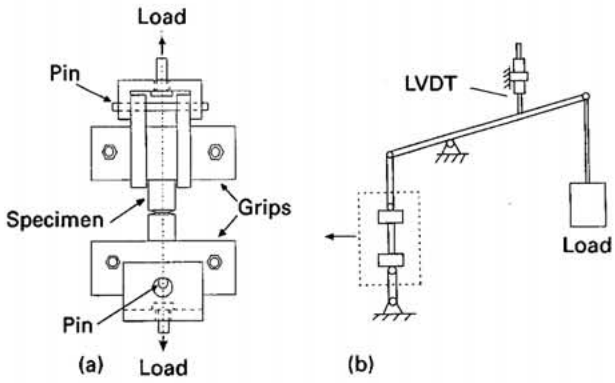

Figure 4 Configuration of craze test rig and grips.

if the gauge length is too long, the measured extension between the gauge length will be largely the creep extension of the bulk and therefore the accuracy of the computed data for the craze zone extension cannot be guaranteed. The chosen gauge length of 40 mm was about twice the specimen thickness and was believed to be of sufficient length to avoid the craze zone being influenced by the grips. The grips and the fixtures were designed in such a way that only a pure tensile deformation was applied to the test piece. Bending and twisting were avoided by using two perpendicular pin axes and two screws as shown in Fig. 4a. Extension in the gauge length was recorded against time by using an LVDT (Linear voltage displacement transducer) as shown in Fig. 4b and the data recorded by a computer.

2.3. Materials and testing procedures

Three different grades of polyethylene supplied by BP Chemicals in the form of slow cooled compression moulded sheets were tested. Some properties of the materials are listed in Table I.

Specimens were annealed before being tested so as to release the residual stresses induced during notch fabrication. After being notched the specimens were sealed into plastic bags and put into hot water at 80 °C for 2 h and then cooled down at a rate of about 7 °C h^{-1}. Tests were started at least 40 h after annealing. Because of the high constraint in the specimen, a craze was produced upon loading, which could be observed as a whitened layer. In most cases, a multiple craze (craze bunching) was generated rather than a single craze. To examine the yielding behaviour and the possible craze mechanisms as well as the coupling effect between the two operating in the craze, some long term dead load tests were terminated and the specimens tested at a constant speed on an Instron testing machine. Also some specimens were tested on the Instron machine to produce a pre-craze before creep testing.

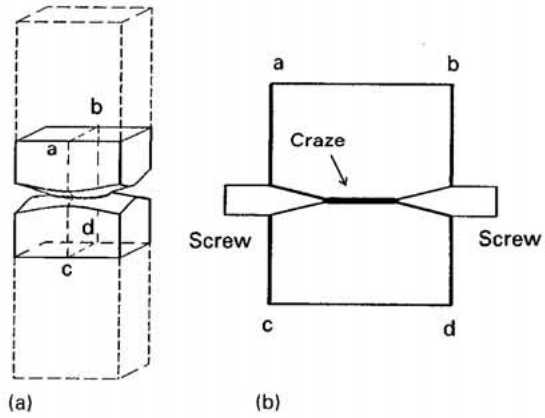

Figure 5 Schematic presentation of partitioning a specimen for SEM examination.

2.4. Micrography

Some selected tests were stopped so as to examine the craze structures by scanning electron microscopy (SEM). The central part of the specimen was sectioned through one of its symmetrical sections to expose the craze generated, as schematically presented in Fig. 5 (a and b). Since the craze is basically elastic immediately after its formation, self tapping screws were used to reopen the craze which gives an approximate way of simulating the loading conditions. The SEM pictures were then taken of the sections.

TABLE I Properties of the polyethylenes

Designation	M_w (kg mol^{-1})	M_n (kg mol^{-1})	Chain branch (per 1000C)	Density (kg m^{-3})
PE1	152	21	approx. 1 butyl	954
PE2	180	18.4	approx. 4.5 butyls	938
PE3	300	13	1.7 butyl + 0.3 ethyl	948

M_w: Weight average molecular weight.
M_n: Number average molecular weight.
C: Carbon (element).

3. Basic mechanical behaviour and failure modes

3.1. Craze zone kinetics and characterization

3.1.1. Constant speed tests

Tests were performed on an Instron testing machine at various speeds so that the time dependent failure behaviour of the crazed materials could be examined. A direct result for a test is its stress against extension curve which includes both the craze thickness and the bulk deformation between grips in the recorded extension. From the comparison between the recorded extension and the simultaneously optically measured craze thickness, it was shown that the bulk deformation was negligible and therefore the recorded extension can be regarded approximately as the craze thickness. A group of such curves for tests of identical PE2 specimens are presented in Fig. 6. The traces vary

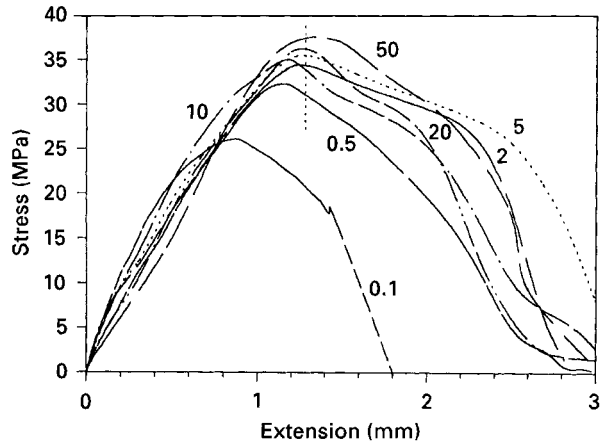

Figure 6 Traces of craze tests at various speeds (Instron) for PE2. The numbers on the figure are the speeds in units of mm min^{-1}.

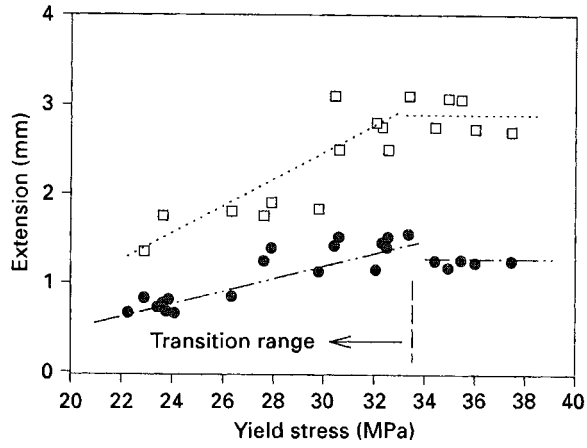

Figure 7 Extension against yield stress for PE2 craze tests (Instron). Key. (□) Delta b at break, (●) Delta c (at yielding).

with testing speed and can be characterized by their yielding stress (maximum stress), extension at yielding, δ_c, and extension at break, δ_b. It is apparent in the figure that although δ_c and δ_b stay almost unchanged at about 1.3 and 3 mm respectively at higher testing speeds, both of them drop remarkably at a low speed of 0.1 mm min^{-1}. These characterizing parameters are plotted in the form of extension against yield stress in Fig. 7 which includes further results of tests at lower speeds. The continuous drop both in δ_c and δ_b as well as the difference between them at lower stresses, corresponding to lower speeds, are in sharp contrast to the plateaus at higher stress levels. These observations infer a constant critical displacement which controls the high stress ductile failures, while for low stress cases the displacement at failure is smaller. Similar test data for PE1 are presented in Figs 8 and 9 for stress-extension curves and as extension against yield stress plots respectively. The extension at yielding

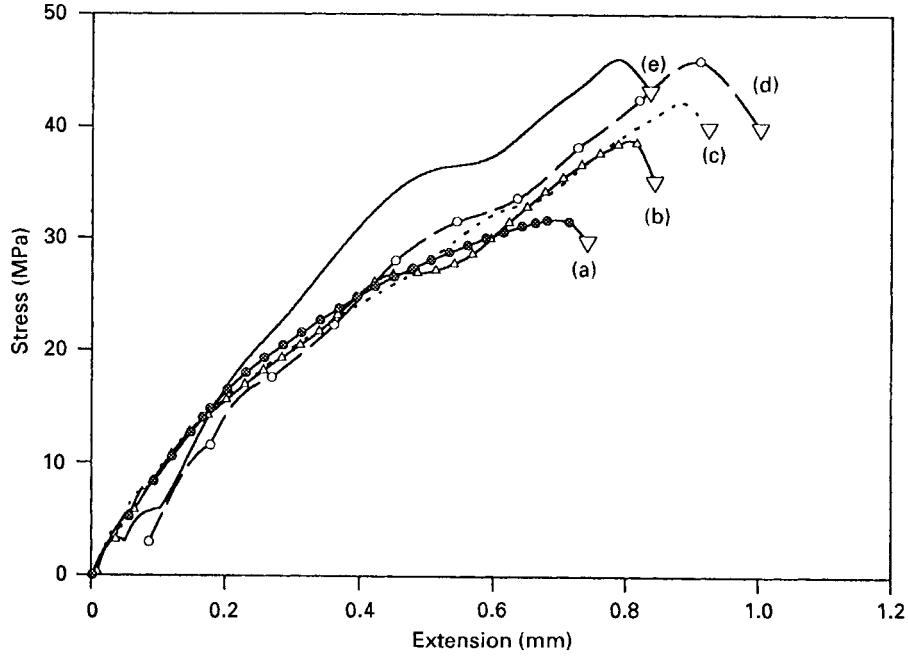

Figure 8 Traces of craze tests for PE1. Speeds of (a) 0.2 mm min^{-1}, (b) 1 mm min^{-1}, (c) 2 mm min^{-1}, (d) 10 mm min^{-1} and (e) 50 mm min^{-1}. The symbol (▽) represents the break point.

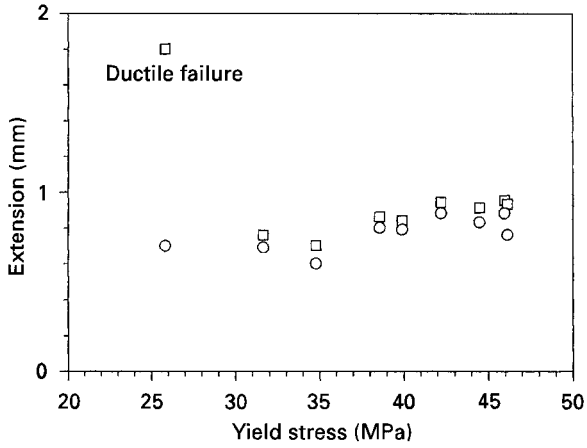

Figure 9 Extension against yield stress for PE1 craze tests. Key: (□) Delta b (at break) and (○) Delta c (at maximum load).

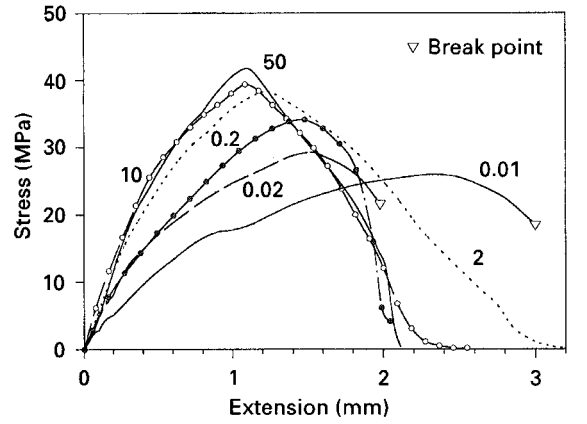

Figure 10 Traces of craze tests at various speeds (Instron) for PE3. The numbers on the figure are the speeds in units of mm min^{-1}.

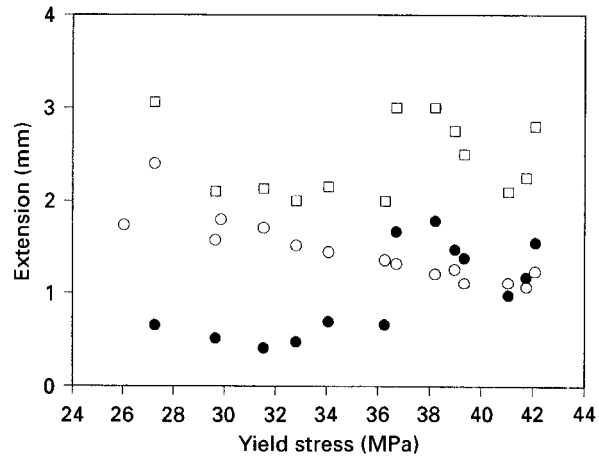

Figure 11 Extension against yield stress for PE3 craze tests. Key: (○) Delta c (at yielding), (□) Delta b (at break) and (●) Delta b – Delta c.

decreases with decreasing speed, and the material always fails in a brittle manner such that specimens break immediately after reaching maximum load.

The situation in Fig. 10 for PE3 is somewhat different from PE1 and PE2 in that the extension at yielding δ_c increases with decreasing speed. This indicates a significant time effect of craze creep and bulk creep at lower speed tests. Nevertheless, from Fig. 11, there is still a clear transition in the plot of extension difference versus yield stress where the lower speed tests (lower stresses) failed suddenly at certain levels of stress with smaller extension after yielding which indicates brittle fractures.

3.1.2. Constant load tests

The direct result for a dead load craze test is a curve of extension against time which includes both the craze thickness and the bulk creep deformation between the grips. For the tough materials PE2 and PE3, satisfactory data have been obtained, but for PE1, the test has proved inapplicable because of the very thin craze which is only produced around the notch tip rather than across the ligament section. The following sections therefore only deal with the two tough materials. To examine the bulk creep deformation, uniaxial tensile creep tests with unnotched specimens were conducted under a stress of 2.5 and 3.16 MPa for PE2 and PE3 respectively. The bulk deformation has been found to be

$$\Delta l = 0.23t^{0.13} \quad \text{for PE2} \tag{1a}$$

$$\Delta l = 0.65t^{0.073} \quad \text{for PE3} \tag{1b}$$

where t has the units of hours and Δl of mm. Since the specimens used in the tests are deep notched, the stresses in the bulk are very low and therefore the creep deformation in the bulk can be assumed to be linear with applied stress. Thus the bulk creep deformation can be expressed as:

$$\Delta l = 0.092\sigma t^{0.13} \quad \text{for PE2} \tag{2a}$$

$$\Delta l = 0.206\sigma t^{0.073} \quad \text{for PE3} \tag{2b}$$

where σ has the units of MPa. The results of the total extension, computed bulk creep deformation and the final craze growth curves for a typical test are presented in Figs 12 and 13 for PE2 and PE3 respectively. Unlike the craze extension, the bulk creep basically follows a power law relation with time and hardly changes from shortly after initial loading. PE2 shows a smaller portion of bulk creep in the total deformation while PE3 has a lower value of time dependent index which results in a rapid decrease with bulk creep.

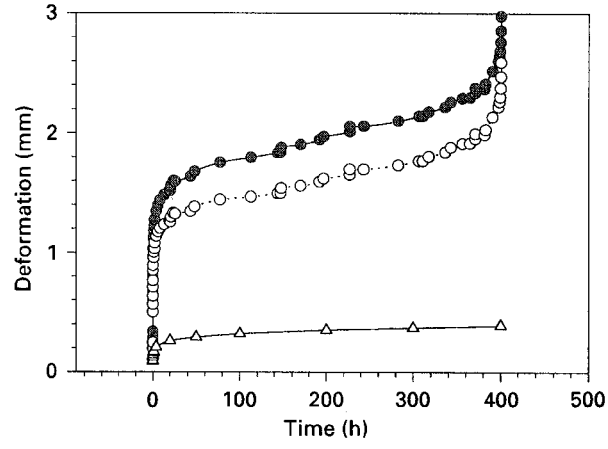

Figure 12 Comparison between curves of (●) total deformation, (△) bulk creep and (○) craze thickness for PE2, (net ligament stress: 16.6 MPa; bulk section stress: 1.92 MPa; gauge length: 40 mm).

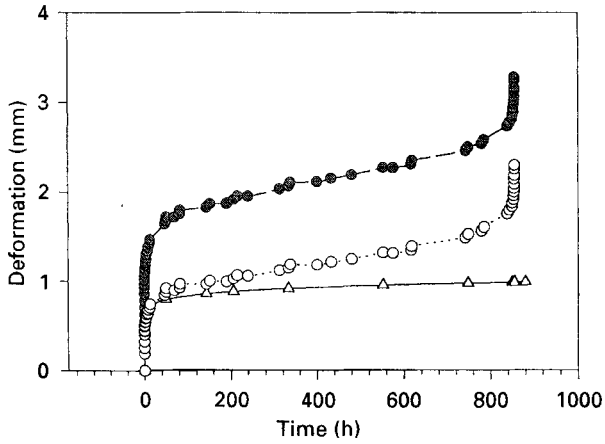

Figure 13 Comparison between curves of: (●) total deformation, (△) bulk creep and (○) craze thickness for PE3, (net ligament stress: 18.48 MPa; bulk section stress: 2.96 MPa; gauge length: 40 mm).

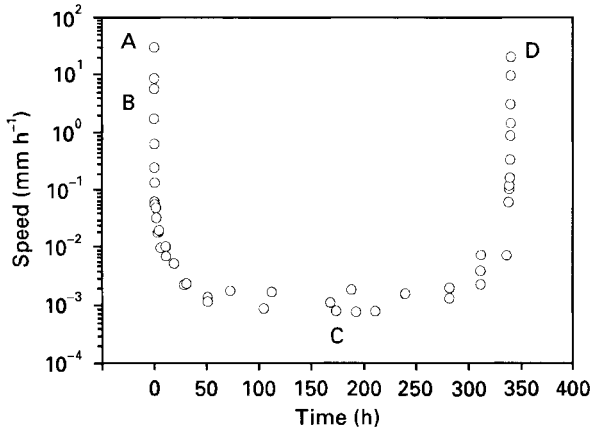

Figure 14 A typical curve of craze zone growth speed against time for PE2 (log-linear).

A typical craze growth speed against time curve is shown in Fig. 14 which is obtained from the craze thickness data by using a local 5 point linear curve fitting. A striking feature of the curve is that the craze speed changes very slowly over most of the time. The U shaped craze speed curve can be divided into two distinct parts AC and CD with speed decreasing and increasing respectively. The minimum speed point C corresponds to the yielding state in which the maximum resistance of the material at that speed is equal to the external load. Although the two parts are roughly equal, the post-yielding part of the curve with increasing speed probably has different deformation mechanisms from the earlier hardening part. There is a competition between the yielding speed and the material resistance under the applied stress and further craze damage and yielding lead to a continuing decrease in load bearing capacity of the material until the final failure.

The curve in Fig. 14 is re-plotted in Fig. 15 in a log–log basis in which the first part of the curve becomes particularly highlighted. It is evident that the major portion of it is a straight line with a small initial steeper portion. The sharp drop in speed at the early stage AB is due to the craze formation immediately upon loading and the part with linear decrease in speed is believed to be caused mainly by the craze

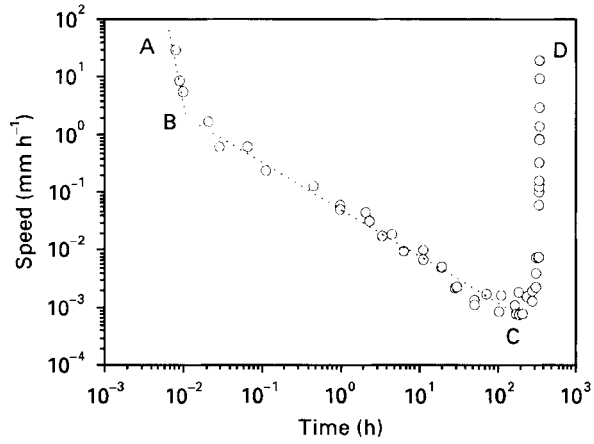

Figure 15 Re-plot of the curve in Fig. 14 on a log–log basis.

creep which should reflect the characteristics of the drawn material in the craze. Despite the fact that the time to yielding increases with decreasing applied stress, the craze zone growth speed of this linear part normalized by the applied stress is found to be uniform for a wide range of applied stress levels as can be seen in Fig. 16 for PE2 where the normalized speed is:

$$\dot{h}_n = 10^{-3} \times 4.6t^{-0.9} \quad \text{(mm/h/MPa)} \qquad (3)$$

The linear correlation in the log–log basis holds in a range of more than 5 decades for both speed and time and for a wide range of applied net section stress. Equation 3, means that the craze zone growth speed is proportional to applied stress but time dependent and is not Newtonian viscous flow as suggested by Brown and Lu [8]. In order to compare the creep behaviour of crazed material and plane stress drawn material, some creep tests were performed using a PE2 sample drawn under a plane stress state from thin tensile specimens of dimensions $100 \times 10 \times 4$ mm. The Sherby–Dorn plots (strain rate ~ strain) of these tests are shown in Fig. 17. The different curves show the differences in the dependence of strain rate on strain for various applied stress levels and the differences between the curves are only a parallel shift. The strain rate as a function of time for these tests is plotted in Fig. 18 and again a unique linear relation which is almost independent of applied stress is found in the log–log basis even though the curves for higher stress levels have slightly less steep slopes. The curve can be expressed as:

$$\dot{\varepsilon} = 10^{-3} \times 7.42t^{-1.03} \quad (\text{h}^{-1}) \qquad (4)$$

It is natural at this stage to reason that the differences between the curves in Fig. 17 solely arise from the initial deformation upon loading which is stress dependent and that there is another mechanism operating during creep which is only a function of time. If the behaviour of the material in the craze zone could be regarded as the same as that of the drawn material produced under plane stress, from Equations 3 and 4, the thickness of the craze zone upon loading could be deduced as:

$$h = \frac{\dot{h}_n \cdot \sigma}{\dot{\varepsilon}} = 0.62\sigma \cdot t^{0.11} \quad \text{(mm)} \qquad (5)$$

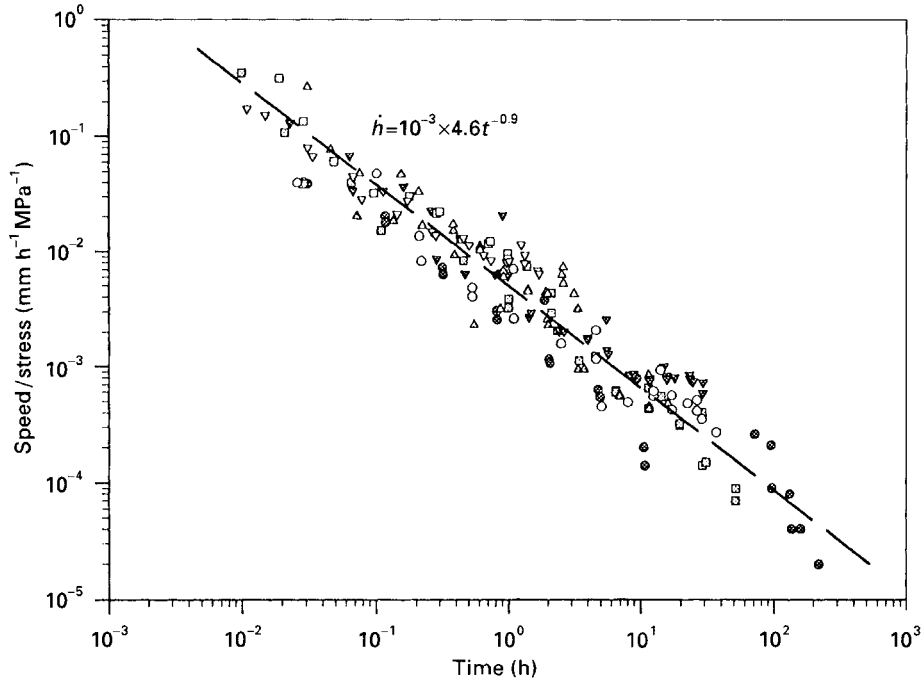

Figure 16 Craze zone speed normalized by applied stress for PE2 at various stress levels of: (●) 15.72 MPa, (⊞) 16.53 MPa, (△) 16.66 MPa, (○) 16.79 MPa, (▼) 18.09 MPa, (△) 20.19 MPa, (□) 20.77 MPa and (▽) 23 MPa.

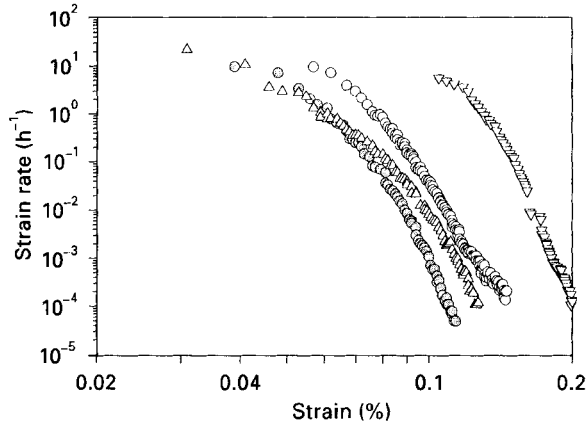

Figure 17 Strain rate versus strain plots (Sherby–Dorn plots) for PE2 material drawn under plane stress state. Key: (◎) 30.6 MPa, (△) 37.5 MPa, (○) 56.9 MPa, (▽) 78.0 MPa.

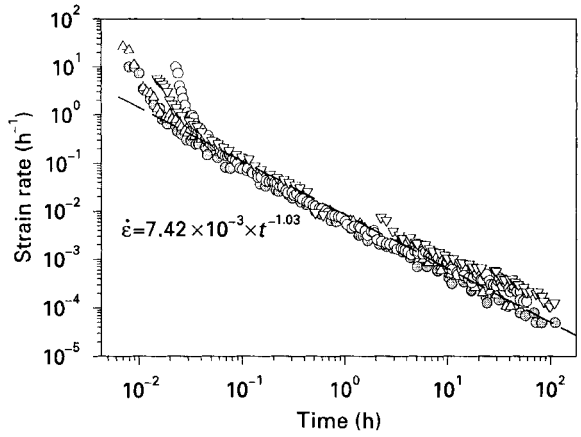

Figure 18 Strain rate as a function of time for PE2 drawn material, Key: (◎) 30.6 MPa, (△) 37.5 MPa, (○) 56.9 MPa and (▽) 78.0 MPa.

It is reasonable that the primordial thickness of a craze zone is proportional to the applied stress, which can also be seen from the initial parts of the curves in Fig. 6, and it increases with time since there is possibly a continuing draw from the bulk, but the results from Equation 5 are too large. For example $h = 15.4$ mm at $\sigma = 15$ MPa and $t = 100$ h. Normally, the craze thickness is less than about 1 mm. This significant difference stems from the fact that the material in a craze zone creeps at much higher speeds than that of the drawn material produced under the plane stress state.

According to Doolittle [18], the viscosity of a material is strongly dependent on the relative free space, and thus we infer that there is an intrinsic distinction between the two materials. In a plane stress drawn material, voids produced before necking are closed completely at room temperature [14], but the material in a craze zone contains a large number of voids, which is due to the overall plane strain constraint of the zone, and thus causes the faster creep speeds.

3.2. Short term failure and long term failure

The testing duration for most of the fixed speed tests performed on the Instron was less than 10 h depending on the testing speed and these tests are called short term tests. For most of the dead load creep craze tests the life time was usually over 10 h depending on the applied stress and the tests are accordingly called long term tests. In these two kinds of test the materials exhibited at different dependence of failure time on applied stress and also a different failure mode.

A comparison of the dependence of time to yielding on net section stress between the long term tests and the short term tests for PE2 is shown in Fig. 19 where the stresses for short term tests are those corresponding to the maximum loads during testing. It is apparent

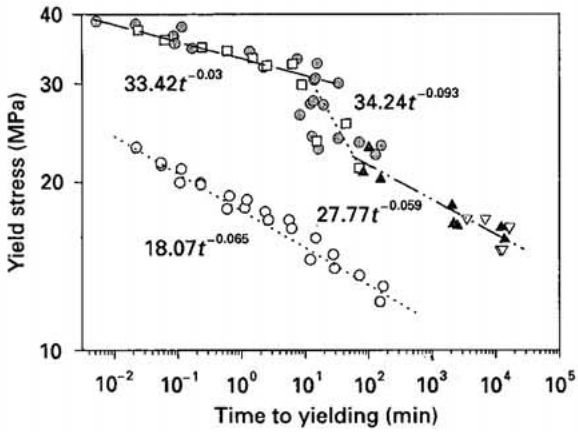

Figure 19 Yield stress against time to yielding for PE2 (PA: plane strain with CDNT specimens; PE: plane stress with thin dumbbell specimens; CS: constant speed tests; CL: constant load tests; R: round ligament specimens; S: square ligament specimens) Key (◍) PA, CS, R, (□) PA, CS, S, (▽) PA, CL, R, (▲) PA, CL, S and (○) PE, CS.

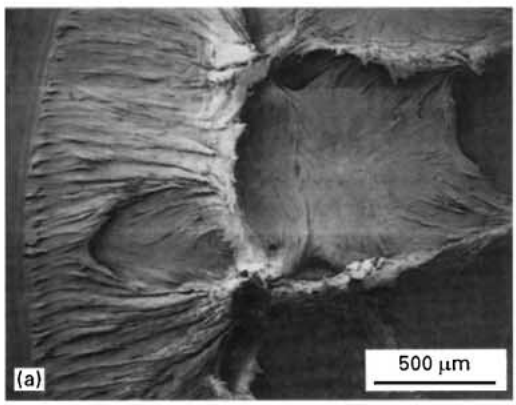

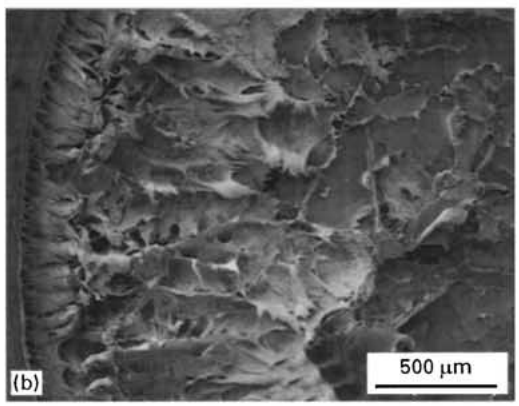

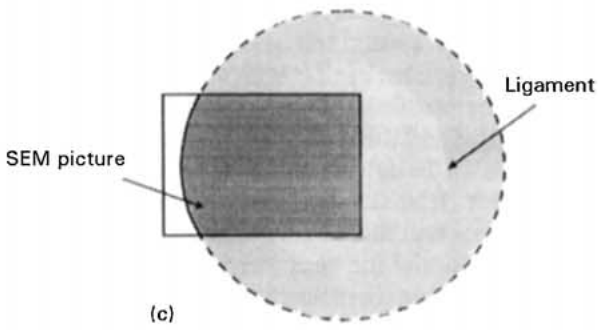

Figure 20 Fracture surfaces for PE2. (a) ductile surface, (b) brittle surface and (c) picture position on the ligament section.

that the data for short term tests at higher stress levels and the data for long term tests follow their own distinct dependence of time to yielding on stress despite the difference in specimen ligament, and there is a clear transition between the two at intermediate stress levels. The difference in time to yielding against stress corresponds to a difference in failure mode. While for short term tests except for those at very low speeds ($< 0.2\ \text{mm min}^{-1}$) the failures are ductile, for all long term tests except for those with high stresses (> 20 MPa) the failures are brittle. The ductile–brittle transition at intermediate stress levels can also be seen in Fig. 7 where the extension at yielding decreases with stress in the lower stress range. The definition of the terms "brittle" and "ductile" are somewhat different from the conventional concepts, which will be discussed and modelled in later sections, and the difference between the two modes can be seen from the fracture surfaces shown in Fig. 20 (a and b) which cover both the boundary area and the central area of the axis symmetrical ligament as defined in Fig. 20c. While the ductile failure surface (a) shows large scale of whitened plastic deformation which could be a result of large scale yielding, the brittle failure surface (b) consists of voids and fine fibrils which could be a combined result of yielding and creep deformation. The morphology of the central area of the brittle surface in Fig. 20(b) is slightly different from that of its boundary area and this may infer a difference in constraint conditions between the areas. Unlike the fibrils standing straight on the brittle surface the stretched material in the craze zone for short term tests shrank significantly after failure without creep induced plastic deformation which usually corresponds to a molecular rearrangement and is not recoverable after testing. The exact failure mechanisms for the two failure modes are complex, but the distinct features of the surfaces for the two modes imply different failure mechanisms. The fact that the transition between the two modes only exists under plane strain conditions as compared with the data of the plane stress state shown in Fig. 19 indicates that the failure modes must be associated with the structure of the craze which is only produced under plane strain conditions. The failure

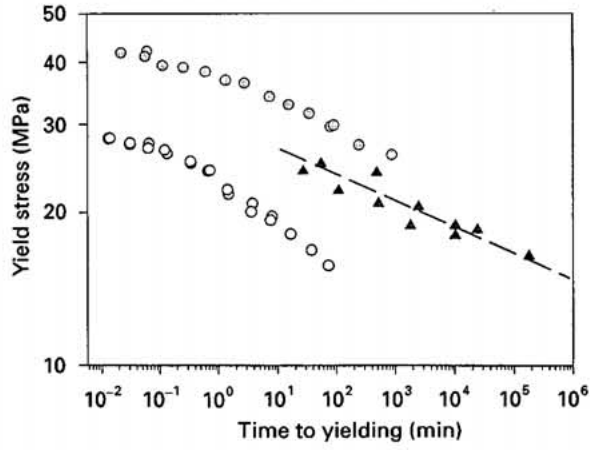

Figure 21 Yield stress against time to yielding for PE3. Key: (○) plane stress at constant speed, (◍) plain strain at constant speed and (▲) plane strain at constant load.

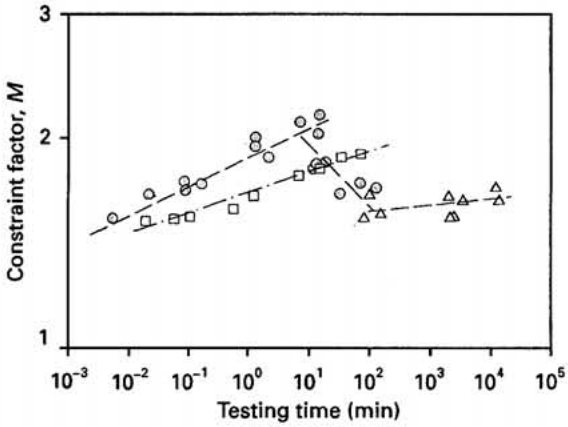

Figure 22 Crack tip constraint factor as a function of testing time. Key: (◎) PE2 constant speed, (△) PE2 constant load and (□) PE3 constant speed.

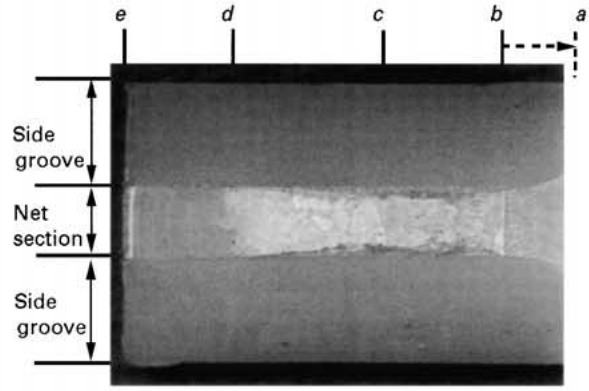

Figure 23 A typical fracture surface for TPB specimens showing three stages of fracture. *b–c*: long term craze failure, *c–d*: short term ductile failure, and *d–e*: rapid crack growth.

mode for PE3 is more complex than that of PE2. Though the short term failure and the long term failure in Fig. 21 follow different dependencies of time to yielding on yield stress, there is no clear ductile–brittle transition. A long term fracture for this material is generally accompanied with a thicker layer of creep induced plastic craze material than a short term fracture.

The difference of the dependence of yield stress on time to yielding between the plane stress state and the plane strain state makes it possible to evaluate the crack tip constraint factor, M, under the plane strain conditions directly from the test data. The factor is defined as the following:

$$M = \frac{\sigma_{y,\text{plane.strain}}}{\sigma_{y,\text{plane.stress}}} \tag{6}$$

Fig. 22 shows the results of M as a function of testing time (time to yielding) for PE2 and PE3, which were calculated from the data shown in Figs 19 and 21 as the ratio of plane strain yield stress to plane stress yield stress. Both materials show an increase in M with loading time which would be expected to promote brittle behaviour. The drop observed in PE2 is presumably associated with the micro voiding associated with the observed change in fracture appearance. For PE3 there is no drop and no change in surface appearance but M does continue to rise.

4. Modelling the crack initiation for slow crack growth

It has been established for high density polyethylenes that crack initiation is followed by a period of slow stable crack growth until final failure. For tougher PE materials such as PE2 and PE3 under plane strain conditions, it has been found that with three point bending (TPB) specimens of moderate laboratory sizes (width = 30–45 mm) and within a laboratory test duration (up to 10 000 h), crack initiation is followed by a crack jump through the crack tip craze zone, a short length of stable crack growth of a ductile type and then an unstable rapid crack growth. A typical fracture surface of this kind is shown in Fig. 23 where *a–b* is the machine notch, *b–c*, *c–d*, and *d–e* are the zones corresponding to the above three stages respectively. The most brittle region *d–e* is a typical rapid crack growth surface without whitening. The whitened region *c–d* is melt like and shows no creep induced plasticity which resembles short term test fracture surfaces. The region *b–c*, which is the region of the initial crack tip craze zone, exhibits fine dimples and fibrils with the length decreasing gradually from the crack tip *b* to the craze tip *c*, which reflects the craze zone profile and also indicates a failure of the fibrils along the craze edges. The sudden failure through the whole craze zone implies that a constant CTOD (crack tip opening displacement) criterion for fracture does not apply in this case. From the point of view of craze degradation, two conditions should be met for the sudden failure through the whole craze zone. One is that the stress is constant along the craze zone and the other is that the load bearing time for different points in the zone is about the same at failure. These conditions can be met if the creep induced stress redistribution time is much shorter than the failure time. From COD (crack opening displacement) and craze length measurements [14], it has been found that for tests of lifetimes over 500 h, it takes a time less than one tenth of the life time for the craze to reach 85% of its final length at failure. This means that for a long term TPB fracture test, the stress redistribution time for these tough PEs is only a small portion of the fracture initiation time. Thus, we can assume that the stress distribution along the craze edges and the stress state in the craze zone of a long term fracture test of any specimen geometry are the same as that in the craze zone of a circumferentially deep notched test specimen, and therefore the fracture initiation time for a fracture test can be predicted by using the craze test data.

With creep induced stress redistribution, the actual stress in a craze zone after redistribution can be estimated by using the concept of a "reference stress". This concept has been pursued by workers on metals and had its origin in the findings of Schulte [19] in that creep analysis of a rectangular beam under uniform bending moment revealed the existence of a particular location in the beam where the stress remained

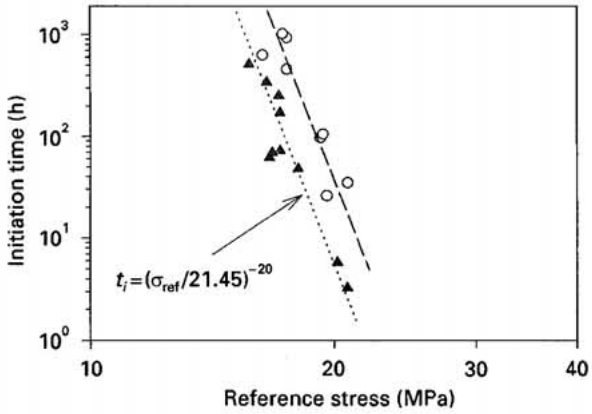

Figure 24 Initiation time against reference stress for PE2 TPB fracture tests compared with craze test results. Key: (▲) Craze test, and (○) TPB fracture.

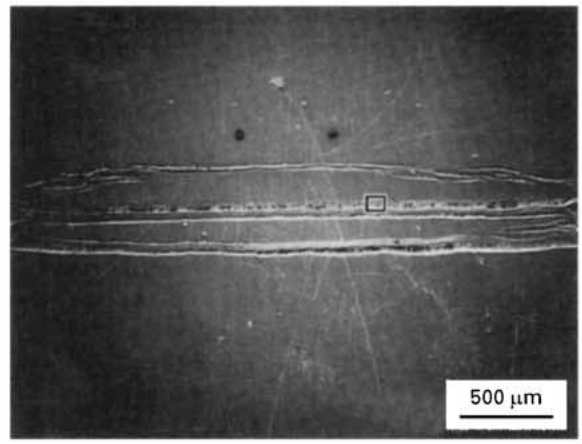

Figure 25 Craze bunching in a typical PE2 specimen.

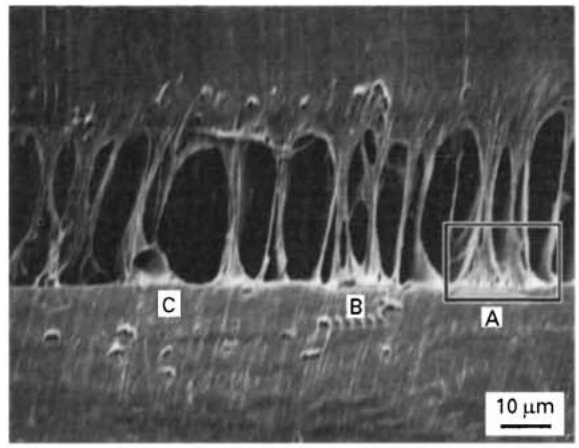

Figure 26 Craze structure for PE2, a single craze thickness showing regularly distributed large cavities and micro voids along craze edges.

invariant during stress redistribution by creep. Schulte postulated that this value of the invariant stress could serve as a reference stress for the whole beam and any uniaxial creep and rupture tests conducted at the reference stress could reproduce the behaviour of the beam. An estimate of the upper bound for the reference stress can be derived from the simple plasticity/creep relationship [20]:

$$\sigma_{ref} = \frac{P\sigma_y}{P_U} \tag{7}$$

where P is the current load, P_U is the rigid-plastic collapse load for the component, and σ_y is the yield stress. The term σ_y/P_U is simply a geometric factor that can be obtained analytically or from model tests. For TPB specimens with $l = 4W$, we have:

$$\sigma_{ref} = \frac{kP}{Wb(1-\alpha)^2} \tag{8}$$

where b is the net thickness, W is the width, α is the crack length ratio, a/W, and $k = 4$ for ideal rigid-plastic bending with hinge at $0.5(W - a)$. Thus from the life time results of the craze tests, $t_f = (\sigma_0/21.45)^{-20}$ for PE2, we have the theoretical relation between crack initiation time and the reference stress as:

$$t_i = (\sigma_{ref}/21.45)^{-20} \text{ (h)} \tag{9}$$

where σ_{ref} takes the units of MPa. Fig. 24 shows a comparison of the reference stress dependence of crack initiation time for TPB fracture tests and the life time for craze tests. The data for TPB fracture tests show some experimental scatter and give a fitting line with a slope almost the same as that of the craze tests. The difference between the two fitting lines is possibly due to the overestimate of the reference stress from Equation 8 which gives the upper bound rather than an exact value of reference stress. Thus, the use of the concept of reference stress and the life time data of craze tests gives a conservative life time prediction for the fracture problems. If σ_{ref} is multiplied by a factor ϕ $(0 < \phi < 1)$, Equation 9 will give a much more accurate prediction.

5. Craze structure and damage process

5.1. PE2

Craze bunching (multiple crazes) occurred in almost all the specimens, and an illustration is shown in Fig. 25. The basic microstructure of the craze is exhibited in Fig. 26 which was taken from the area defined in Fig. 25. The porous crazed material consists of regularly distributed large cavities separated by fibrils (actually warped films) of drawn material with small voids around the fibril roots which can be clearly seen from the high magnification picture Fig. 27 (boxed area in Fig. 26). Less voids can be detected on the wall of the fibrils and this may lead the fibrils to be stronger in the central portion than in their roots. The existence of micro voids may be favourable for long term processes such as molecular disentanglement leading to material damage. This is confirmed by the sequential SEM pictures taken at different intervals from the same specimen as shown in Fig. 28 (a and b). The specimen had been under a loading condition controlled by using screws and the screw penetration was increased with time in order to compensate for the stress relaxation. The picture in Fig. 28 (a) was taken 700 h later than the one in Fig. 26. It shows a failure at point E and damage of different extent at points B, C and the upper root of fibril A. The fracture at point

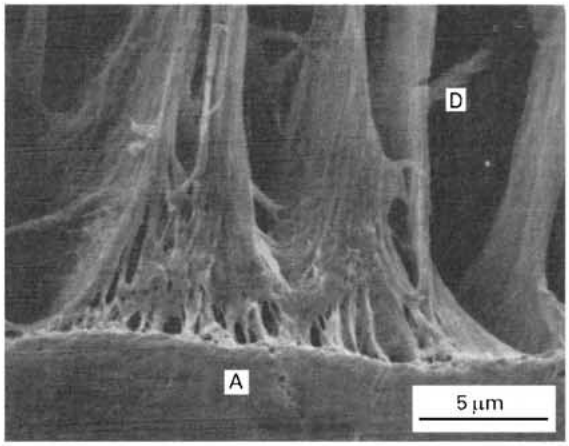

Figure 27 A high magnification view of a fibril root area taken from the defined area in Fig. 26.

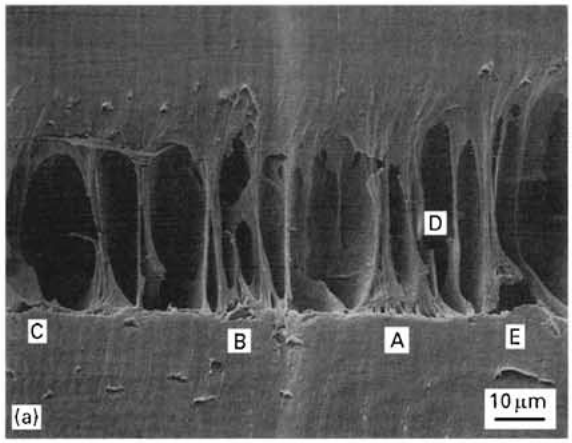

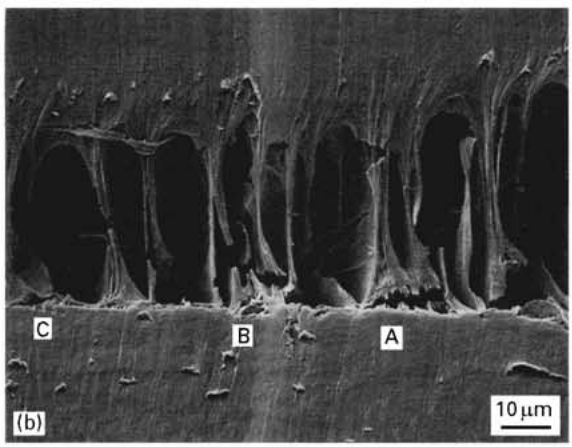

Figure 28 Different stages of damage process in a PE2 craze.

D was caused by a sharp scratch as shown in Fig. 27 and should not be regarded as a creep failure of the film. Further damage at points *B* and *C* is recorded in Fig. 28(b). A complete failure at point A is observed where there is a high density of small voids. The large crack in the wall of the warped film above between *A* and *B* is probably a result of tearing caused by the failure in the adjacent areas rather than a failure of the film by creep.

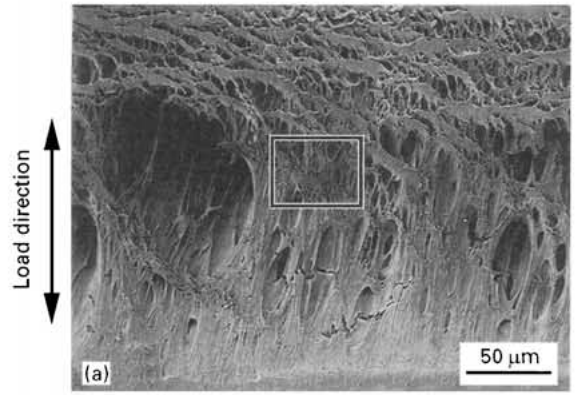

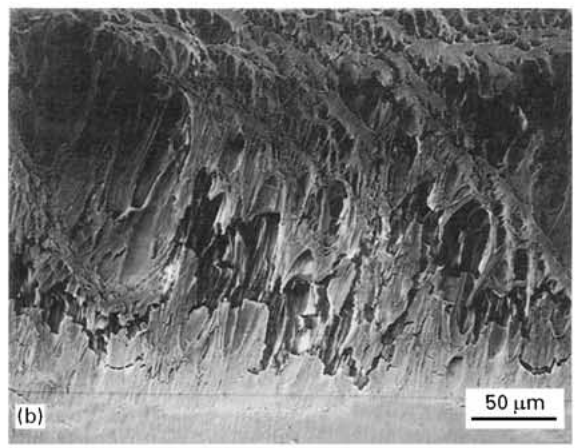

Figure 29 Craze structure for PE3 and micro cracks in the craze. (a) the whole thickness of the craze; (b) crack propagation along the boundary of a large hole.

5.2. PE3

PE3 has been proved to have thicker crazes and much higher resistance to slow crack growth than PE2 [14]. This is attributed to the distinct microstructure of its craze. Unlike the craze structure of PE2 in Fig. 28 (a and b) which has a regular distribution of large ellipsoidally shaped cavities with much smaller voids along the craze edges, the much thicker craze in PE3 as shown in Fig. 29 (a), which was also taken from a typical craze bunch, contains randomly distributed ellipsoidally shaped cavities or voids with size ranging from less than 1 μm to about 100 μm. With the help of a closer view in Fig. 30 taken from the central boxed area of Fig. 29 (a) it is shown that despite the various sizes of the voids, all the longer axes of the ellipsoidals are aligned with the load direction (the load direction is somewhat out of the plane of the partitioned section which causes the stripes in the upper area in Fig. 29 (a)). The honeycomb structure with isolated cavities is a network with linking walls in various thickness. Since the voids are randomly distributed, the weakest areas of the craze should also be randomly distributed rather than along craze edges as in PE2. A curved crack can be identified in the lower central area in Fig. 29 (a) which was further extended as shown in Fig. 29 (b). It is interesting to note that fracture took place along the lower boundary of the largest hole (lower left) which happened to be an area with high density of small voids as can be seen in Fig. 29 (a).

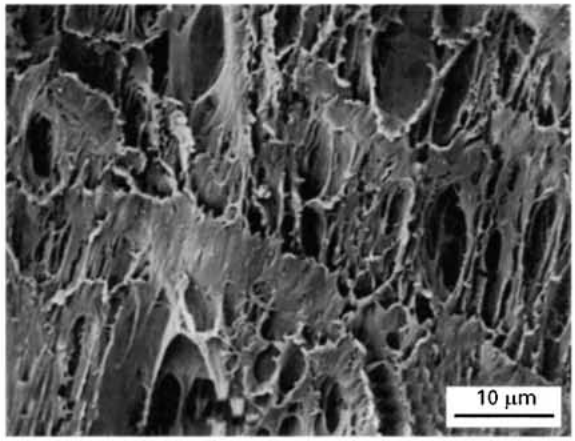

Figure 30 Honeycomb structure of the craze showing randomly distributed cavities for PE3.

5.3. Discussion

It is important to notice the difference in structure of a craze between the central parts of fibrils or common walls of cavities and the roots of fibrils or the joints of walls. While the former are under quasi-plane stress conditions, the latter have higher constraints and are under plane strain dominant conditions with a high density of voids. This observation is helpful in understanding the failure modes of short term tests and of long term tests. Different events may take place after the craze formation process for short term fractures and for long term fractures. The instantly formed craze zone is basically elastic in nature as far as the fibrils or films are considered if the applied stress is under the short term strength. This has been confirmed by a series of short term tests where the whitened craze layer (0.2–1.2 mm in thickness) produced before the maximum load was closed immediately after unloading. If a specimen is loaded beyond the maximum load point but before failure, craze deformation will be partly recovered and a permanent craze zone (layer) will be formed. Thus the maximum load point corresponds to a yielding process. The short term failure may be accomplished by the breakdown of the fibrils across their central part since there is a relatively lower yield stress under plane stress conditions. The melt like whitened fracture surface is probably due to the elastic contraction of the broken films and the micro voids near the fibril roots (the craze edges). For a long term fracture where the applied stress is much lower than its short term strength, two independent processes take place simultaneously after the formation of the craze zone upon loading. One is the ductile creep deformation of the fibrils under constant stress with a creep speed decreasing with time as shown previously which is much higher than the creep speed of the material drawn under a pure plane stress state. During the creep process, the original elastic fibrils gradually become plastic. The other process, namely brittle damage, takes place in the region of the fibril roots where there is a high density of micro voids. The damage is due to several micro events. One of them is the disentanglement of the molecules in the amorphous region for which the rate should be strongly dependent on the density of molecule side branches. Another possible event is the chain scission which takes place on the molecule chains bearing high stress due to the local stress concentration. These micro events are unlikely to happen in the central part of the fibrils formed where the chains are highly oriented and aligned and there is less free space for disentanglement. With the damage process continuing, the fibrils break subsequently at their roots and with the number of fibrils decreasing, the actual stress in the remaining fibrils eventually reach their yield stress at the corresponding speed, which is approximately the minimum speed on the craze growth against time curve.

Once the yielding point is reached, three different mechanisms operate jointly, namely, ductile creep (at very low speed for a long term fracture due to work hardening), brittle damage and yielding. Although the yielding depends on the damage extent, it is the yielding mechanism that controls the final failure. The failure along craze edges is most likely as we have already observed in the tests since there is a high density of micro voids and a high constraint in these areas. Due to randomly distributed voids in the craze in PE3, the high density micro void areas are also randomly distributed and thus micro cracks induced by brittle damage may be in areas other than the craze edges which is clearly seen in Fig. 29 (b).

6. Long term fracture resistance evaluation

Like the short term fracture toughness studies in which fracture criteria are established for material quality control and design purposes, the long term damage fracture study of the materials comes to its ultimate topic of fracture resistance evaluation. The unique characteristic of the long term fracture behaviour of polyethylenes is that the materials cannot be characterized by a single valued fracture parameter due to their time dependent nature. A straight forward approach for the long term fracture resistance evaluation in the current research is the application of the test data of applied stress against time to yielding as shown in Fig. 19. Generally, the long term fracture resistance of a material can be expressed in terms of its stress and time dependent yielding as the following equation:

$$\sigma = A t_y^{-n} \tag{10}$$

or

$$t_y = \left(\frac{\sigma}{A}\right)^{-1/n} \tag{11}$$

where $A > 0$ and $n \geqslant 0$ are material constants, t_y and σ are time to yielding and the applied stress.

Equation 11 is more convenient for interpreting the physical implications of the parameters A and n. A is the stress level at which the material considered fails at unit time (minute) and can be termed as *the general*

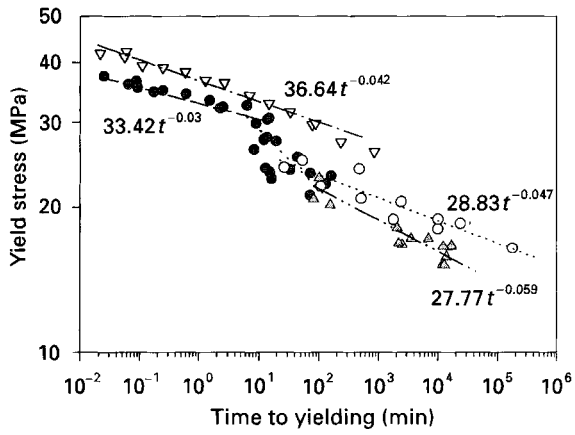

Figure 31 Comparison of yield stress against time to yielding between PE2 and PE3. Key (▽) constant speed, PE3, (○) constant load, PE3, (●) constant speed, PE2 and (△) constant load, PE2.

load bearing capacity parameter. The index n which scales the time dependence of the material's behaviour and is termed as *damage evolution index* with $n = 0$ corresponding to time independent fracture for which A corresponds to a critical fracture stress. With the definitions of the parameters A and n, materials can thus be compared and graded in terms of long term fracture resistance by evaluating these parameters. A material with better long term fracture resistance has a higher A and a lower n. A comparison of PE2 with PE3 is presented in Fig. 31. Apparently, PE3 has a better long term fracture resistance with the value A and n of 28.83 and 0.047 respectively compared to 27.77 and 0.059 for PE2. An extrapolation of t_y with a value of 50 years which is commonly used as a design life time for pipe-lines gives an applied stress of 10.13 and 12.92 MPa for PE2 and PE3 respectively. If the applied stress for PE2 is the same as the 12.92 MPa calculated for PE3, its life time is only 298 days. We also calculated n for the brittle high density polyethylene PE1 by using the concept of reference stress and by using the data of time to crack initiation against applied stress intensity factor K [14]. A high n value of 0.125 was obtained which corresponds to the lowest long term fracture resistance.

7. Conclusions

The following conclusions can be drawn from the tests and the analyses:

(1) The specimen of circumferentially deep notched tensile geometry has been proved to be suitable for producing a craze in tough polyethylenes which resembles the zone at a crack tip. The advantages of this geometry over other fracture specimen geometries are that it produces a craze zone across the ligament under a near plane strain state without shear lips on the fracture surface, and it enables the analyses of the craze behaviour to be carried out under a definite stress level rather than in a time dependent stress field. It also provides information directly on craze kinetics rather than an indirect method by using drawn materials.

(2) It was discovered that craze zones in polyethylenes are composed of honeycombs rather than fibrils. That is to say that the drawn material in a craze is mostly in a form of warped film under a biaxial stress state rather than fibrils under uniaxial tensile stress.

(3) There is a big difference in craze micro structure between PE2 and PE3. While the former has a craze consisting of large cavities regularly distributed with small voids along the craze edges, the latter produces a craze with cavities of various sizes distributed randomly in it. This difference may be attributed to the difference in their molecular structures.

(4) Long term damage failure and short term fracture correspond to different dominant failure mechanisms. While the short term failure is accomplished by the breakdown of fibrils (warped films) across their central parts due to the overall craze yielding, the long term failure is caused by an accumulation of brittle damage in areas such as the fibril roots and film joints where there is a high density of micro voids and a high constraint which produces local hydrostatic stress.

(5) The data of life-time against applied stress obtained from craze tests can be used to predict the crack initiation time for structures via the concept of a reference stress, which gives a conservative prediction.

(6) Polyethylene materials can simply be graded in terms of long term fracture resistance by comparing the *general load bearing capacity parameter* and the *damage evolution index* which can be obtained directly from craze tests data.

Acknowledgement

The authors are grateful to BP Chemicals Ltd for the financial support of this project. In particular, thanks are due to Drs E Q Clutton and L J Rose of the company for their helpful comments.

References

1. J. M. GREIG, P. S. LEEVERS and P. YAYLA, *Engng. Fracture Mech.* **42** (1992) 663.
2. P. YAYLA and P. S. LEEVERS, *ibid.* **42** (1992) 675.
3. J. G. WILLIAMS, "Fracture mechanics of polymers", (Ellis Horwood, Chichester, UK, 1987).
4. J. G. WILLIAMS and G. P. MARSHALL, *Proc. R. Soc. Lond.* **A342** (1975) 55.
5. N. BROWN, J. DONOFRIO and X. LU, *Polymer* **28** (1987) 1326.
6. P. S. LEEVERS, *Int. J. Fract.* **73** (1995) 109.
7. X. LU and N. BROWN, *J. Mater. Sci.* **26** (1991) 612.
8. N. BROWN and X. LU, *Int. J. Fract.* **69** (1995) 371.
9. M. J. CAWOOD, A. D. CHANNEL and G. CAPACCIO, *Polymer* **34** (1993) 423.
10. L. J. ROSE, A. D. CHANNEL, C. J. FRYE and G. CAPACCIO, in Proceedings of 8th International Conference on Deformation, Yield and Fracture of Polymers, Churchill College, Cambridge, 11–14 April, 1994 (Institute of Materials, London, 1994) p. 57.
11. N. BROWN and X. WANG, *Polymer* **29** (1988) 463.
12. M. K. V. CHAN and J. G. WILLIAMS, *Int. J. Fract.* **23** (1983) 145.
13. M. F. KANNINEN, P. E. O'DONOGHUE, C. F. POPELAR, C. H. POPELAR and V. H. KENNER, *GRI-93/0106, Final Report*, Vol. 2, (Gas Research Institute, USA, 1993).
14. D.-M. DUAN, PhD thesis, University of London, (1996).

15. N. NISHIO, S. IIMURA, M. YASUHARA and F. NAGATANI, in Proceedings of 9th Plastic Fuel Gas Pipe Symposium, New Orleans, 1985, (American Gas Association, New Orleans, USA, 1985) p. 29.
16. M. FLEIBNER, *Kunststoffe German Plastics* **77** (1987) 16.
17. J. LAI and A. BAKKER, *Polymer* **36** (1995) 93.
18. A. K. DOOLITTLE, *J. Appl. Phys.* **22** (1951) 1471.
19. C. A. SCHULTE, in ASTM STP60, (American Society for Testing and Materials, Philadelphia, PA, 1960) p. 895.
20. R. G. SIM, PhD thesis, University of Cambridge, (1968).

Received 19 May
and accepted 4 August 1997